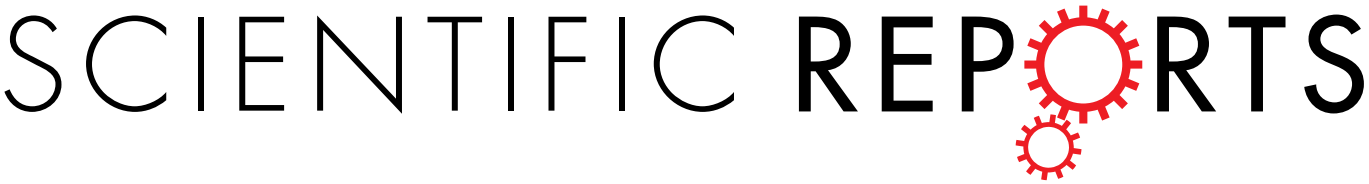

OPEN

Channel based generating function approach to the stochastic Hodgkin-Huxley neuronal system

Received: 08 December 2015
Accepted: 09 February 2016
Published: 04 March 2016

Anqi Ling[1,2], Yandong Huang[3], Jianwei Shuai[3] & Yueheng Lan[1,2]

Internal and external fluctuations, such as channel noise and synaptic noise, contribute to the generation of spontaneous action potentials in neurons. Many different Langevin approaches have been proposed to speed up the computation but with waning accuracy especially at small channel numbers. We apply a generating function approach to the master equation for the ion channel dynamics and further propose two accelerating algorithms, with an accuracy close to the Gillespie algorithm but with much higher efficiency, opening the door for expedited simulation of noisy action potential propagating along axons or other types of noisy signal transduction.

Hodgkin and Huxley first proposed a classical way to deterministically characterize neuronal dynamics based on a quantitative analysis of experimental results[1]. The phenomenological Hodgkin-Huxley equations treat the neuron membrane as a capacitor with a set of continuous parallel channels for the passage of ions, and the permeability of the neuronal membrane determines ion-specific currents. Each ion channel has four subunits, being independent and each either open or closed. The conductance is determined by the fraction of ion channels in an open state in which all subunits are open. With further indepth investigation, stochasticity is found to play an important role in neuronal dynamics[2–4] and the cooperative behaviors in biological neuronal networks, such as pattern formation[5], synchronization[6–8] and coherence[9–11] which are of great importance to the understanding of generation and functioning of several neural diseases[5]. Individual voltage- or ligand-gated ion channel randomly alternates between open and closed states which turns out to be a major source of noise in neuronal activity, the so-called channel noise[12,13], and contributes to the generation of spontaneous action potentials[14,15], variability in spike timing[16], firing coherence[10], and the regularity of spontaneous spiking activity[11]. The nonlinear amplification of synaptic signal makes up another source of noise, which also greatly influences the membrane potential fluctuations[17–20].

Channel noise has been identified to be essential to neuronal dynamics and coding, and has been extensively studied in recent years in a variety of neural systems, like the auditory nerve by cochlear implants[21], and in cerebellar granule cells[22]. It turns out that channel noise has measurable effects under normal conditions, which not only makes a big difference to the initiation and propagation of action potentials, such as firing irregularity[23,24], spiking threshold and firing rate[25,26], but also enhances sub-threshold signal above certain magnitude[27].

As mentioned above, ion channels are subject to random changes among a number of possible channel conformations. The stochastic kinetics of ion channels could be defined as a Markov chain, with discrete phase space states where each state in the chain represents a particular configuration of the ion channel. The random transition of an ion channel from one state to another just depends on its current state in the Markov assumption, which can be exactly simulated by the Gillespie algorithm[28]. This algorithm tracks the number of channels in each state at each time point on one trajectory, and many trajectories are computed for well converged statistics. It is both accurate and simple to use but computationally demanding especially in the large channel number limit and hard to analyze mathematically which may be essential for an indepth understanding of neuronal dynamics.

One commonly used alternative is the Langevin approach which treats channel noise as a Gaussian one, first proposed by Fox and Lu[29,30]. However, in comparison with the exact Gillespie algorithm, the original Langevin approaches could not accurately capture the stochastic channel dynamics. One computes subunit fractions with noise in which the subunits of K^+ and Na^+ channels are identical (Identical LA)[29,30]. An improvement was put forward through rescaling the noise intensity with an empirical factor by Huang *et al.* (Rescaled LA)[31]. Another one

[1]Department of Physics, Tsinghua University, Beijing 100084, China. [2]Collaborative Innovation Center of Quantum Matter, Beijing 100084, China. [3]Department of Physics and Institute of Theoretical Physics and Astrophysics, Xiamen University, Xiamen 361005, China. Correspondence and requests for materials should be addressed to Y.L. (email: lanyh@mail.tsinghua.edu.cn)

adds noise to the channel fractions (Fox-Lu channel based LA)[29]. Nevertheless, the channel fractions obtained from the corresponding numerical computation may be out of the biologically meaningful interval [0, 1], especially at small channel numbers. The Cholesky decomposition was used to treat the stochastic terms (Orio LA)[32], known as channel-based Langevin approach with unbounded state fractions. To bound the channel state fractions within [0, 1], a reflection boundary condition was supplied[33]. A more accurate version was later proposed by Huang *et al.*, who designed a restoration scheme to put the changes of state fractions back to the SDEs after a truncation (Truncated-Restored LA)[34]. It has been pointed out that the bounded Truncated-Restored Langevin approach and the unbounded Orio Langevin approach exhibit equally good, and also the best approximations to the exact Markov dynamics among these Langevin approaches[35]. However, as reviewed by Huang *et al.*, despite for small channel numbers, currently proposed Langevin approaches cannot accurately replicate the statistical properties of the Markov HH model even at large channel numbers, calling for a better approach to the stochastic HH dynamics[35].

Nevertheless, a Markov chain is completely described by a master equation, a group of ordinary differential equations for the probabilities of discrete states[36]. There are many approximate approaches developed for solving master equations in a variety of biochemical networks, for instance, the noisy signal transduction network[37–39]. Lan *et al.* demonstrated the equivalence of the field theoretic formulation to the generating function approach which is based on mapping an enormous set of master equations (ODEs) into one single partial differential equation (PDE)[40], and has been applied in a plethora of cases[41]. In the current work, we design a new hybrid scheme for the computation of noisy neuron dynamics based on the generating function formulation, and in addition propose two accelerating algorithms for improved efficiency. Our method produces statistics of stochastic action potential that agree well with exact ones in different situations no matter if the channel number is small or large, the input current is constant or noisy. It is computationally efficient compared to the Gillespie algorithm and many variants of Langevin approach. When the channel number is small, it produces results that match those from Gillespie computation while all Langevin approaches fail or are not accurate. The current approach balances well accuracy and efficiency and opens the door for large-scale computation in stochastic axonal dynamics.

Results

Implementation with generating function. As discussed in the Methods section, the propagation of the action potential along an axon is described by a stochastic version of the HH equation, which could be transformed to a PDE for the generating function of the channel system. As the transition rates of the K^+ channel state depends on V, the expression below is an analytic approximate solution of the generating function equation

$$\begin{aligned}\Psi &= \prod_{i=0}^{4}\Psi_i = \prod_{i=0}^{4}(x_0 f_{0i} + x_1 f_{1i} + x_2 f_{2i} + x_3 f_{3i} + x_4 f_{4i})^{m_i} \\ &= \sum p(n_0, n_1, n_2, n_3, n_4)\, x_0^{n_0} x_1^{n_1} x_2^{n_2} x_3^{n_3} x_4^{n_4}\end{aligned} \tag{1}$$

which would become exact if the time dependence of V has been known. $(n_0, n_1, n_2, n_3, n_4)$ denotes one possible distribution of the K^+ channels with the probability $P(n_0, n_1, n_2, n_3, n_4)$. Here m_i is the number of channels in the ith channel state at $t = t_0$ and the probability f_{ij} satisfies the equation

$$\frac{d\mathbf{f}}{dt} = A_K \mathbf{f}, \tag{2}$$

where A_K is the transition matrix of the K^+ channel states.

A similar expression can be written down for the Na^+ channel

$$\Phi = \prod_{j=0}^{7}(y_0 p_{0j} + y_1 p_{1j} + y_2 p_{2j} + y_3 p_{3j} + y_4 p_{4j} + y_5 p_{5j} + y_6 p_{6j} + y_7 p_{7j})^{n_j}. \tag{3}$$

Here n_j is the number of Na^+ channels in the jth state at $t = t_0$ and p_{ij} satisfies the equation

$$\frac{d\mathbf{p}}{dt} = A_{Na} \mathbf{p}, \tag{4}$$

where A_{Na} is the transition matrix of the Na^+ channel states, and p_{7j} is the probability that during the evolution time the jth Na^+ channel state makes a transition to the 7th channel state, i.e., the open state.

The mean value and standard deviation of the number of open K^+ and Na^+ channels are computed from the generating function:

$$\langle N_{K^o}\rangle = \sum_{i=0}^{4} m_i f_{4i},\ \sigma_{N_{K^o}{}^2} = \sum_{i=0}^{4} m_i f_{4i}(1 - f_{4i}) \equiv \Gamma_1, \tag{5}$$

$$\langle N_{Na}{}^{o}\rangle = \sum_{j=0}^{7} n_j p_{7j},\ \sigma_{N_{Na^o}{}^2} = \sum_{j=0}^{7} n_j p_{7j}(1 - p_{7j}) \equiv \Gamma_2. \tag{6}$$

Since $N_K{}^o$, $N_{Na}{}^o$ are random variables, the voltage V is also random. But, we could speculate that the distribution of V would be narrow during a small time interval if starting with a definite value. However, with time evolution the distribution of the random variable V becomes wider and wider. If σ_V which is the standard deviation

of V is larger than a given width, then we should sample a new set of numbers $\{m_K\}$, $\{m_{Na}\}$ to describe the K^+ and Na^+ channel states according to the probability distribution given by the generating function, and reinitialize f and p. In this way, V could be always approximated by the local $\langle V\rangle$ at any time.

In the Methods section, a linear noise approximation is used to estimate σ_V. A new sampling is made whenever $\sigma_V > (D_V)_T$, where $(D_V)_T$ is a chosen membrane voltage threshold. Specifically, sampling of K^+ and Na^+ states according to the multi-nomial distribution, based on the probabilities given by f and p, may be decomposed into successive binomial ones. Take the sampling of K^+ states for example. First, we could sample the number m_{i4} of which the ith channel state makes a transition to the 4th, i.e., the open state, with the transition probability f_{4i}. After this has been done, Ψ_i becomes ${x_4}^{m_{i4}}(x_0 f'_{0i} + x_1 f'_{1i} + x_2 f'_{2i} + x_3 f'_{3i})^{m_i - m_{i4}}$, where $f'_{ki} = \frac{f_{ki}}{f_{0i}+f_{1i}+f_{2i}+f_{3i}}$, $k = 0, 1, 2, 3$.

Similarly, one by one we could get the transition numbers from the ith to the 0, 1, 2, 3th channel state respectively. After all samplings are done, Ψ_i will be $x_0^{m_{i0}} x_1^{m_{i1}} x_2^{m_{i2}} x_3^{m_{i3}} x_4^{m_{i4}}$. The generating function of the sampled state would be $\Psi = \prod_{i=0}^{4} \Psi_i = \prod_{i=0}^{4} x_0^{m_{i0}} x_1^{m_{i1}} x_2^{m_{i2}} x_3^{m_{i3}} x_4^{m_{i4}}$, and we could get a distribution of the K^+ channel state $\{n'_0, n'_1, n'_2, n'_3, n'_4\}$, where $n'_i = \sum_{k=0}^{4} m_{ki}$. The sampling of Na^+ states could be done in a similar way.

Besides that, the sampling of membrane voltage may be needed. The assumption that V behaves according to a random normal distribution with mean $\langle V\rangle$ and standard deviation σ_V seems reasonable. Nevertheless, according to our experience, it is comparatively convenient to fix the width of the distribution as taking $dV = 0.1\,mV$ in the sampling of V.

As a summary, we arrive at the following procedure:

(1) Initialize the number of each K^+ and Na^+ channel state $\{m_K\}$, $\{m_{Na}\}$ at time t, and set f and p the identity matrix.
(2) Solve the ODEs for f, p, $\langle V\rangle$, and σ_V.
(3) Integrate to time t' until the inequality $\sigma_V \le (D_V)_T$ breaks, sample a new set of channel numbers in each K^+ and Na^+ channel state with the probabilities computed from the generating function, and sample a new V based on the normal distribution $N(\langle V\rangle, \sigma V)$. Take σ_V to be 0 and reinitialize f and p.
(4) Check if $t \ge T$. Yes, stop computation. No, go back to (2).

Though the above scheme is precise and can fully capture the dynamics of the system, it involves many ODEs and during the evolution many channel numbers will be sampled, so that the calculation is cumbersome. We propose two approximations to accelerate the algorithm under the premise of accuracy. Accelerating algorithm 1 is designed to reduce samplings of channel numbers. In accelerating algorithm 2, even the number of ODEs is much reduced.

Accelerating algorithm 1. As V just depends on the number of open ion channels, we need only to sample the open channel numbers with the known transition probability of each state to the open state when the voltage width limit is reached at step (3) above. Take the K^+ channel as an example. After we sample open channel numbers as discussed above, the generating function turns to

$$\Psi = x_4^{m'} \prod_{i=0}^{4} (x_0 f'_{0i} + x_1 f'_{1i} + x_2 f'_{2i} + x_3 f'_{3i})^{m_i - m_{i4}} \tag{7}$$

where $m' = m_{04} + m_{14} + m_{24} + m_{34} + m_{44}$ is the total number of open potassium channels.

As the probability flow in $(x_0 f'_{03} + x_1 f'_{13} + x_2 f'_{23} + x_3 f'_{33})^{m_3 - m_{34}}$ is close to that in $(x_0 f'_{04} + x_1 f'_{14} + x_2 f'_{24} + x_3 f'_{34})^{m_4 - m_{44}}$ and $m_4 - m_{44}$ is small, one can take the critical step to merge the two factors $(x_0 f'_{03} + x_1 f'_{13} + x_2 f'_{23} + x_3 f'_{33})^{m_3 - m_{34}} (x_0 f'_{04} + x_1 f'_{14} + x_2 f'_{24} + x_3 f'_{34})^{m_4 - m_{44}}$ into one $(x_0 f''_{03} + x_1 f''_{13} + x_2 f''_{23} + x_3 f''_{33})^{m'_3}$, where $(m_3 - m_{34}) f'_{i3} + (m_4 - m_{44}) f'_{i4} = m_3 f''_{i3}$, and $m'_3 = m_3 - m_{34} + m_4 - m_{44}$, which determines f'_{i3} in a unique way.

Accelerating algorithm 2. If the channel number is large enough, a reasonable approximation to binomial distribution is given by a normal distribution. And as we know, if X and Y are independent random variables that are normally distributed, then their sum is also normally distributed, with its mean being the sum of the two means, and its variance being the sum of the two variances. So, if all the channel numbers are large, we can take the generating function as $(x_0 f_0 + x_1 f_1 + x_2 f_2 + x_3 f_3 + x_4 f_4)^m$, where m is the total number of K^+ channel. In this case, as above, we can just sample the number in the open channel state when the voltage width limit is reached at above step (3), and the generating function turns out to be $x_4^{m'} (x_0 f'_0 + x_1 f'_1 + x_2 f'_2 + x_3 f'_3)^{m - m'}$ after the sampling. As time goes by, after the next sampling the generating function becomes ${x_4}^{m_4} (x_0 f''_0 + x_1 f''_1 + x_2 f''_2 + x_3 f''_3)^{m - m' - m_{41}} (x_0 f'^{\prime}_0 + x_1 f'^{\prime}_1 + x_2 f'^{\prime}_2 + x_3 f'^{\prime}_3)^{m' - m_{42}}$, where $m_4 = m_{41} + m_{42}$. Same as accelerating algorithm 1, the latter two terms have similar probability flow, and can be merged into one multi-nomial form.

Similar procedure could be applied to the Na^+ channel.

Accelerating algorithms 1 and 2 need only to sample the open ion channels, while the full generating function approach updates all. What's more important is that the number of variables of the ODEs for f and p is much reduced in algorithm 2 which further reduces the computation time compared to algorithm 1. Hence, we would use the accelerating algorithm 2 to effectively reduce computation load.

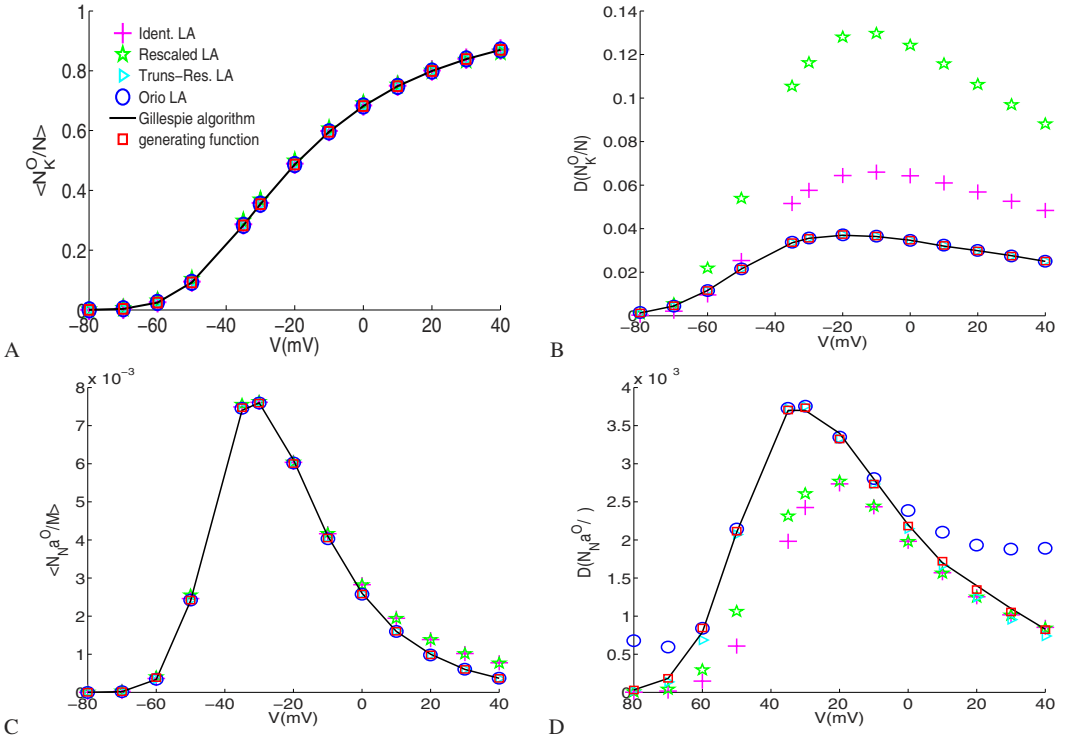

Figure 1. The means and standard deviations of the fraction of open channels with fixed membrane voltage. Results for the K^+ channel (**A**,**B**) and for the Na^+ channel (**C**,**D**). The total number N of the K^+ channel is 180, and of the Na^+ channel $M = 540$. The current I is set to $0\,uA/cm^2$.

Here we compare statistics of observables obtained from the generating function approaches with those obtained from the Gillespie algorithm and five Langevin approaches (Identical LA, Rescaled LA, Fox-Lu channel based LA, Orio LA, Truncated-Restored LA). The number of Na^+ channels maintains three times that of K^+ channels in the simulation. Data are saved at every 0.01 ms.

Open Channel statistics. When the membrane voltage is fixed at a preset level, we measure the electric current and check how the neuron reacts to changes with different membrane potentials[42]. Here we compute the means and standard deviations of the open fraction of sodium and potassium channels under voltage clamp to study the dependence on membrane-patch voltage V. They were calculated over 100000 realizations using the Gillespie algorithm and Langevin approaches, each simulation was run for a total of 100 ms. The numbers of open sodium and potassium channels are collected at the final time point.

Figure 1 shows that as membrane voltage increases, the mean open fraction of the K^+ channel increases and saturates at 1, while that of the Na^+ channel increases first and then decreases, maximizing at $V \sim -30\,mV$. As mentioned above, the opening and closing rates for "activation" subunits and "inactivation" subunits respond oppositely to the change in membrane voltage. As membrane voltage increases, the transition to the open state becomes fast with four identical n subunits in any K^+ channel. But the activation of three m subunits and one h subunit works heterogeneously to jointly determine the channel state of Na^+ channel, so that the transition rate does not monotonically increase.

We see from Fig. 1 that the mean fractions of open channels calculated from the four Langevin approaches are quite similar to the results obtained from the exact Gillspie algorithm. The Truncated-Restored LA replicates the standard deviation, whereas, the standard deviation of potassium currents is overestimated by the two subunit-based LAs, and the standard deviation of sodium currents is underestimated by the two subunit-based LAs and the Truncated-Restored LA, while overestimated by Orio LA. Obvious deviations from the exact ones are found in the two subunit-based LAs.

The results obtained by the generating function approach and by the Gillespie calculation match very well with each other not only for the mean fractions of open channels but also for their deviations. Indeed, under voltage clamp, the generating function result is exact. All subunits in the K^+ channel are identical by assumption, we can show that the generating function will be a multi-nomial $(x_0 f_0 + x_1 f_1 + x_2 f_2 + x_3 f_3 + x_4 f_4)^N$, if starting from a particular state, where N is the total number of K^+ channels. Hence, the mean value and the standard deviation of open K^+ channels are given by eq. (5). The stationary probability distribution is derived from

$$\frac{d\mathbf{f}}{dt} = 0 \tag{8}$$

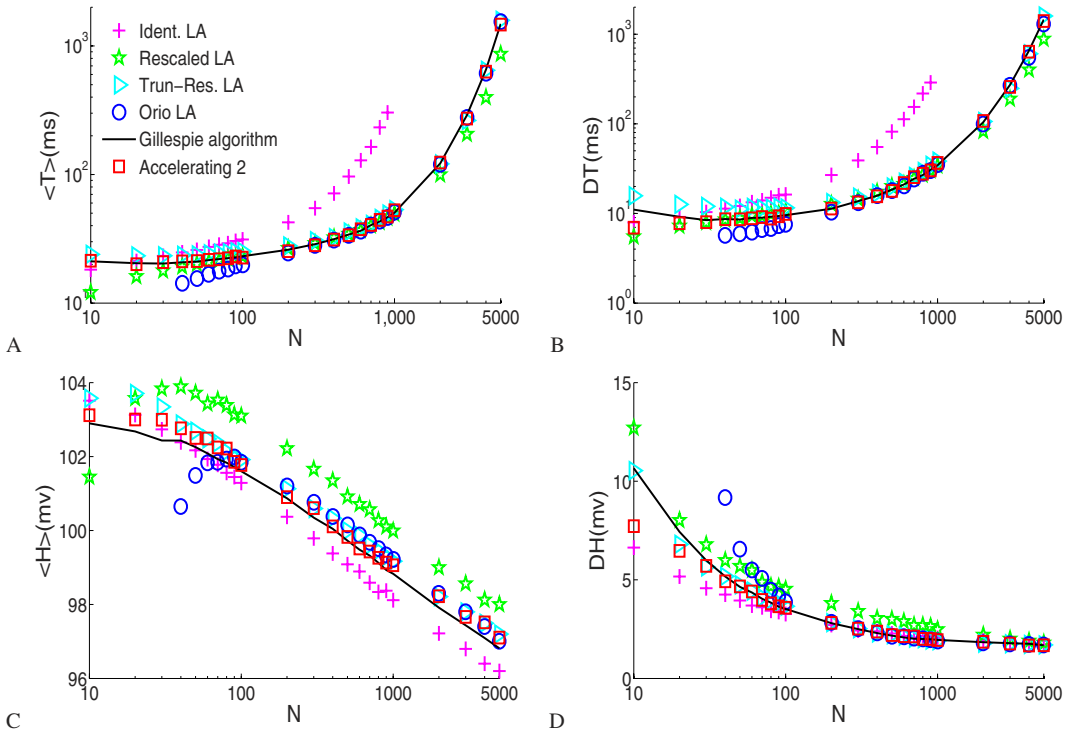

Figure 2. Comparison of the means and the standard deviations of first 10000 interspike intervals and spike amplitudes as a function of the total number of potassium channels, where $I = 0\,uA/cm^2$.

which gives the mean and standard deviation of the open K^+ channel as $\frac{N_K{}^o}{N} = f_4$ and $\sigma\left(\frac{N_K{}^o}{N}\right) = \left(\frac{f_4(1-f_4)}{N}\right)^{1/2}$, where f_4 is $\frac{\alpha_n^4}{(\alpha_n+\beta_n)^4}$. Similarly, the stationary probability distribution for the Na^+ channel is calculated from

$$\frac{d\mathbf{p}}{dt} = 0 \tag{9}$$

which gives the mean and standard deviation of the open Na^+ channel as $\frac{N_{Na}{}^o}{M} = p_7$ and $\sigma\left(\frac{N_{Na}{}^o}{M}\right) = \left(\frac{p_7(1-p_7)}{M}\right)^{1/2}$, where $p_7 = \frac{\alpha_m^2\alpha_h}{(\alpha_m+\beta_m)^3(\alpha_h+\beta_h)}$.

It can be concluded that the mean fractions of open channels are independent of the total channel numbers, and the standard deviations are proportional to $\left(\frac{1}{N}\right)^{1/2}$ or $\left(\frac{1}{M}\right)^{1/2}$, while these quantities depend on the voltage V implicitly.

Spike statistics with no current input. Neuronal signaling study involves measuring and characterizing how stimulus signal propagates, indicated by the neuron action potentials or spikes. Particularly, the statistical study of action potentials is vital to describe and analyze neuronal firing. For example the lengths of interspike intervals (ISIs) often vary randomly but encode important information[43].

An action potential is triggered once the voltage is beyond a threshold V_T for the deterministic HH neuron, giving a spike. Here $V_T = -60\,mV$ is considered. The spike amplitude H is defined as the difference from the peak voltage to the threshold in membrane potential. Considering the absorption of action potentials in the stochastic channel dynamics, a fully developed spike is identified only when the voltage goes up to at least $-30\,mV$ after going beyond the threshold V_T, and shoots back downward below the resting level. That is, the spike has a minimal amplitude H_0 to be $30\,mV$. The interspike interval T is defined as the time interval between two successive spike peaks.

Figure 2 shows the statistical properties of the first 10000 successive spikes for N ranging from 10–5000, in which the input current I is 0. These simulations show that the rates and amplitudes of spiking activity obtained in the accelerating algorithm 2 and the Gillespie algorithm match well. Spiking events become increasingly rare as channel number increases, because the membrane dynamics tends to converge to its deterministic limit gradually in which large voltage fluctuations become increasingly rare while spiking events are mainly driven by large channel noise, and spike amplitude tends to decrease.

We can see from Fig. 2A that the spiking rates obtained from the accelerating algorithm 2 and from the Gillespie algorithm match well at both small and large channel numbers. The threshold for the voltage fluctuation controls the spike frequency and should be carefully chosen in the generating function scheme. The mean ISIs

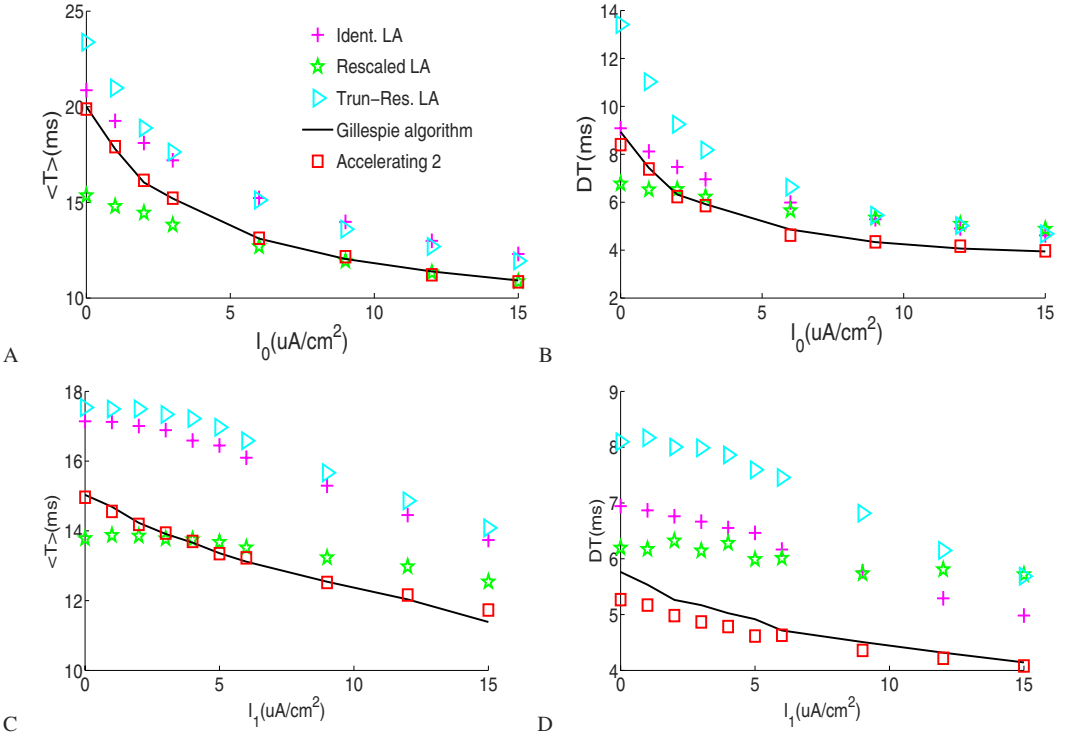

Figure 3. (**A**,**B**) Comparison of the means and standard deviations of the first 10000 interspike intervals as a function of I_0 for $I_1 = 0\, uA/cm^2$. (**C**,**D**) Comparison of the means and standard deviations of the first 10000 interspike intervals as a function of I_1 for $I_0 = 3\, uA/cm^2$. Here the total number N of K^+ is set to 18.

from the Rescaled LA tend to be much shorter than those from the Gillespie algorithm, while in the Identical LA they tend to be longer when channel number $N > 40$ and much longer at big channel numbers. A possible source for these differences between the two subunit-based Langevin approaches is that the noise term added to the subunit fractions should not be of the uncorrelated, zero mean Gaussian type. The results produced by the two channel-based Langevin approaches are in good quantitative agreement with those by the Gillespie algorithm. Nevertheless, there are still some discrepancies at small channel numbers, and the Orio LA breaks down at channel number less than 40. In general, other than the Identical subunit LA, the mean amplitudes calculated from these methods are bigger than that from the Gillespie algorithm, while the discrepancies are minimal between the results from accelerating algorithm 2 and the Gillespie algorithm.

Interspike interval statistics with noisy current input. We study the spiking response to synaptic noise and discuss the statistics of the interspike intervals under a range of current conditions. The noisy current I is of the simple form $I_0 + I_1\xi$[44] here, where ξ is a Guassian white noise with zero mean and unit variance. I_0 refers to the DC level. Due to the additive white noise term $I_1\xi$ which represents the combined effect of a continuous barrage synaptic noisy inputs that neurons in cortical and other neural systems receive, the action potentials may become more fluctuating[44].

Figure 3 plots the means and standard deviations (left and right columns, respectively) of ISIs with different noisy current levels for the Langevin approaches, Gillespie algorithm and accelerating algorithm 2 with small potassium channel number $N = 18$. As a fact, at such a small channel number, the Orio LA breaks down. As the DC level is increased, spiking events become more frequent as shown in Fig. 3A where there is no synaptic noise input and the channel noise reduces its impact on spike timing. Likewise, under a constant DC input, spiking rate increases with the increase of the intensity of the synaptic noise as Fig. 3C suggests. We see that the means and the standard deviations of ISI given by the Gillespie algorithm and accelerating algorithm 2 for different current inputs agree extremely well. Nevertheless there are still some discrepancies between the Langevin approaches and the Gillespie algorithm.

Figure 4 shows results under two different synaptic noisy current levels with large potassium channel number $N = 1800$, for which the Identical subunit LA breaks down. There are observable discrepancies between these LA approaches at low DC level without input noise as shown in Fig. 4A, in which channel noise still accounts for major effect on the regular firing, just like Fig. 2 suggests. As I_1 increases just by $1\, uA/cm^2$, the mean ISI is much reduced, which is particularly evident at low DC level. The agreement between the accelerating algorithm 2 and the Gillespie calculation is still very good. In general, noisy stimuli help reduce the mean ISI and have a significant effect on spike firing especially for large channel number at low DC level.

Membrane Voltage statistics. The membrane voltage statistics are calculated from an ensemble of voltage paths. Figure 5 shows the probability distribution for the membrane voltage at time t = 0.6 ms computed from

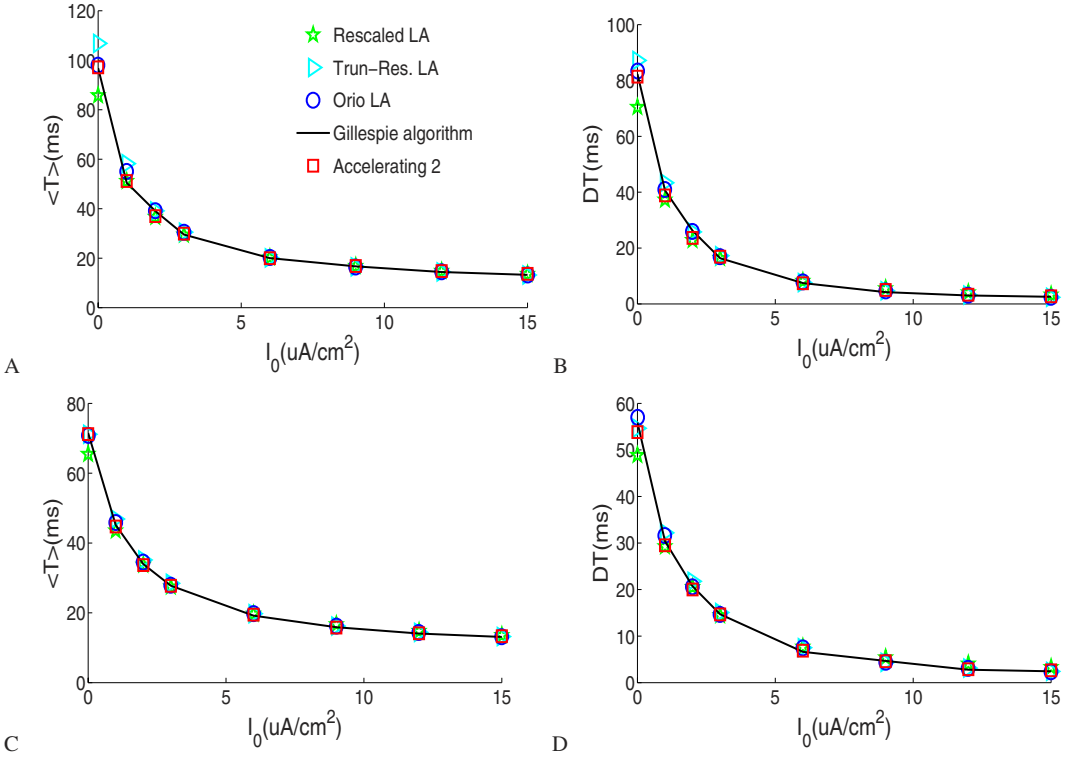

Figure 4. Comparison of the means and standard deviations of the first 10000 interspike intervals as a function of I_0. (**A**,**B**) Results for $I_1 = 0\, uA/cm^2$. (**C**,**D**) Results for $I_1 = 1\, uA/cm^2$. Here the total number N of K^+ is set to 1800.

10000 runs of the Gillespie algorithm, of the three channel-based Langevin approaches, and of three generating function approaches with the same initial fractions of channel states. Fox-Lu channel based LA is less accurate and slower than Orio LA and Truncated-Restored LA, thus we did not show its computation results in previous discussion.

The results show that our generating function approach captures the distribution function very well when compared with the Gillespie algorithm at two different channel numbers. We can see from Fig. 5A that the membrane voltage distribution ranging from -70–$42\, mV$ is close to a Gaussian centered around $V = 27\, mV$, whereas Langevin approaches give nonzero probability only when membrane voltage is larger than $-12\, mV$. While in Fig. 5B the distribution has two peaks around $-68\, mV$ and $+27\, mV$, which Langevin approaches fail to reveal. Because the initial numbers of open K^+ and Na^+ channels are not zero, and the initial fractions of the open K^+ and Na^+ channels are the same in Fig. 5A,B, there is supposed to be a spike for any voltage path near $t = 0.6\, ms$ as shown in Fig. 5C, where the membrane voltage is more likely bigger than a minimal spike value. However, what's interesting is that as the number of K^+ channels decreases to 15, the bistable state appears as shown in Fig. 5B, where another peak locates near $V = -68\, mV$ while the high peak is considerably lower than that in Fig. 5A. From Fig. 5D, we can see that the membrane potential may fail to rise to a value larger than $-30\, mV$ and quickly fall to the resting level. This observation suggests that the strong channel noise at small channel numbers may sometimes undermine rather than promote spike firing.

Computation efficiency. Finally, the computational time of these approaches is summarized in Fig. 6A for the case with no input current. Simulations with Matlab were run on a 3.07 GHz quad core Intel Core i7 processor.

Figure 6A shows that generating function approaches are considerably faster than the Gillespie algorithm, particularly for larger channel numbers. The consumed time grows linearly with the number of ion channels in the Gillespie algorithm, depending on the average time between reactions, which can be very small for large channel numbers, while in the generating function approach the computing time remains more or less constant. Channel numbers are irrelevant to the efficiency of the Langevin approach. The two subunit-based Langevin approaches take the same least time compared to others, and the Truncated-Restored LA spends more time mainly for the calculation of root square of the diffusion matrices than the Orio LA. In total, accelerating algorithms 1, 2 are faster than the channel-based LAs, and the generating function approach is faster than the Truncated-Restored LA.

Although the threshold of the membrane voltage width we take empirically monotonically decreases as shown in Fig. 6B, which is consistent with the fact that as channel number increases, channel noise tends to have less and less effect on spike firing. To guarantee the accuracy enough samplings have to be taken, which leads to an extremely slow increase of the computation time in the generating function approach with the total channel

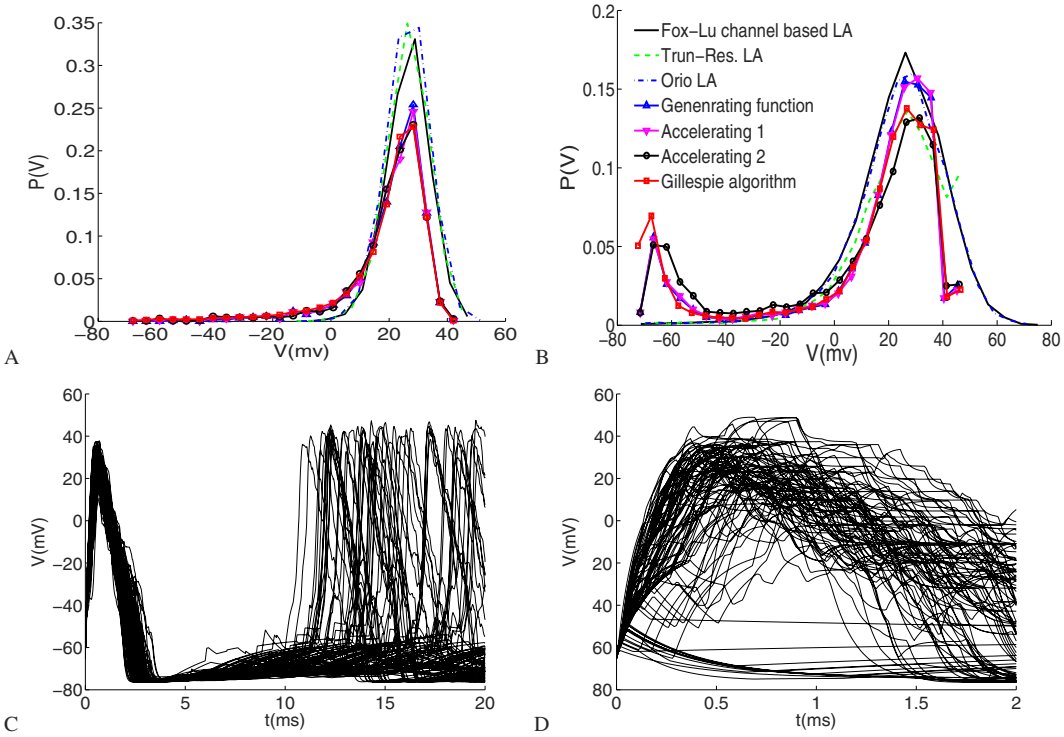

Figure 5. (**A**,**B**) Comparison of the probability distributions of membrane voltage at t = 0.6 ms. (**C**,**D**) The first 100 voltage paths using Gillespie algorithm. (**A**,**C**) The total K^+ channel number N is 60, and results are given with the initial condition $\{m_K\} = \{20, 16, 12, 8, 4\}$, $\{m_{Na}\} = \{40, 32, 28, 24, 20, 16, 12, 8\}$ by the generating function approach, accelerating algorithm 1 and the Gillespie algorithm, while $\{m_K\} = \{56, 4\}$, $\{m_{Na}\} = \{258, 8\}$ by accelerating algorithm 2, and with the initial fractions of K^+ channel $\{5, 4, 3, 2, 1\}/15$, of Na^+ channel $\{10, 8, 7, 6, 5, 4, 3, 2\}/45$ by the three channel based Langevin approaches. (**B**,**D**) The total K^+ channel number N is 15, and results are given with the initial condition $\{m_K\} = \{5, 4, 3, 2, 1\}$, $\{m_{Na}\} = \{10, 8, 7, 6, 5, 4, 3, 2\}$ by the generating function approach, accelerating algorithm 1 and the Gillespie algorithm, while $\{m_K\} = \{14, 1\}$, $\{m_{Na}\} = \{43, 2\}$ by accelerating algorithm 2, and with the initial fractions of K^+ channel $\{5, 4, 3, 2, 1\}/15$, of Na^+ channel $\{10, 8, 7, 6, 5, 4, 3, 2\}/45$ by the three channel based Langevin approaches.

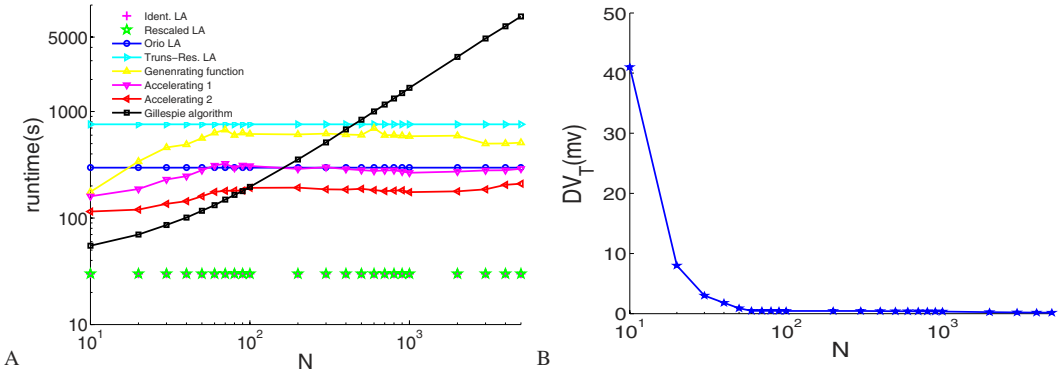

Figure 6. (**A**) Comparison of computing time. The computation is done over a time interval of 40 *s* with a time step of 0.01 *ms*. (**B**) The threshold of the membrane voltage width $(DV)_T$ for different K^+ channel numbers N.

number N. When N is no more than 100, the channel noise seems to be dominating and we choose not to sample membrane voltage.

Discussion

In this work, we applied the generating function approach to the study of stochastic dynamics of the HH model which is a typical Markovian system, accounting for channel shot noise embedded in the evolution of the discrete ion channel states. We designed a numerical scheme to efficiently solve for the generating function, taking into account the channel noise and voltage fluctuations. At the smooth evolution step, due to the peakedness of the membrane voltage distribution at short times, the random voltage is replaced by its mean and hence the channel

state distribution is approximated by a product of multinomial distributions. However, samplings for ion channel states and voltage are needed when a preset width limit of the voltage distribution is reached, which can be estimated with the linear noise approximation. Furthermore, the procedure of how to sample channel numbers from the generating function is explained in detail. In order to make the computation more efficient, we also proposed two accelerating algorithms in which only the number of the open ion channels are sampled since the time evolution of the voltage only depends on this number. The accelerating algorithm 2 further reduces the number of equations by employing a multinomial distribution to approximate the channel states.

Results are compared for different approaches: the generating function, the Gillespie algorithm and the Langevin approaches. We calculated the stationary statistics of the fraction of open channels under voltage clamp. The generating function in this case can be solved exactly for the stationary distribution, and thus the exact expression for the mean and standard deviation of the two open channel states are obtained, whereas most Langevin approaches either overestimate or underestimate the conductance fluctuations except the Truncated-Restored LA. Meanwhile, we studied statistics of action potential spikes at different channel numbers in response to constant and noisy current inputs. Compared to the Gillespie simulation with cumbersome computation, our approach produces result directly in an efficient way. Through our analysis of the statistics of the membrane voltage, it seems that the results from accelerating algorithm 2 match well with those obtained with the Gillespie algorithm, but with much higher efficiency.

It is interesting that with the initial distribution of the ion channel state set up properly, bistable state appears at a particular time when the total channel number is small, which the Langevin approaches fail to reveal. Overall, our simulation results show that the generating function approach provide statistically accurate approximation to the neuronal spiking dynamics for any channel number, while Langevin approaches even break down in some cases.

Finally, we compare the computing time with different numbers of K^+ channels ranging from 10 to 3000, and pointed out that the accelerating algorithms take much less time than the exact Gillespie algorithm, and are also faster than channel-based Langevin approaches. With an empirical selection of the threshold for the membrane voltage width, the new scheme has an accuracy comparable to the Gillespie computation.

Overall, the results from these simulations suggest that the generating function approach is an accurate and fast approximation for discrete-state Markov chain models. In spite of the complexity and nonlinearity of the noisy action potential propagating along an axon, we expect a good performance of the current technique in the study of the neuronal dynamics. An extension of the current technique to the investigation of noisy signal transduction on other types of networks should also be possible.

Methods

The discrete HH model. According to the HH model which regards the cell membrane as a capacitor, the membrane potential V is governed by

$$C\frac{dV}{dt} = I - (I_{Na} + I_K + I_L) \tag{10}$$

where $C = 1\ uF/cm^2$ is the membrane capacitance, and I is the membrane current. I_{Na}, I_K, I_L are the currents of the sodium, potassium, and leakage channels, respectively, and given by

$$\begin{aligned} I_{Na} &= g_{Na}(V - E_{Na}), \\ I_K &= g_K(V - E_K), \\ I_L &= g_L(V - E_L), \end{aligned} \tag{11}$$

where $E_{Na} = 50\,mV$, $E_K = -77\,mV$, $E_L = -54.3\,mV$ are the reversal potentials of the sodium, potassium, and leakage channels, respectively; $g_L = 0.3\,ms/cm^2$, g_{Na}, g_K are their conductances.

As well known, there are four identical and independent n subunits for each K^+ channel and three identical and independent m subunits and one h subunit for each Na^+ channel. Here a single subunit can be in one of the two configurations, open (O) or closed (C) at time t. They convert to each other in a random way more explicitly,

$$C \underset{\beta_i(V)}{\overset{\alpha_i(V)}{\rightleftharpoons}} O \tag{12}$$

where α_i, β_i are voltage-dependent opening and closing rates, and i denotes different types of subunits.

Only when these subunits are all open in a channel, is the channel open. Generally, one defines the conductance based on the fraction of open channels. The K^+ conductance is $g_K = \overline{g_K} f_K$, where f_K is the fraction of K^+ channels that are open, and $\overline{g_K}$ is the maximal conductance of potassium channels. With the knowledge of open channel number ${N_K}^o$ among the total number N_K for K^+ channels, f_K is given by $\frac{{N_K}^o}{N_K}$, where $\overline{g_K} = 120\,ms/cm^2$, $\overline{g_{Na}} = 36\,ms/cm^2$. Similar expressions hold for Na^+ channels. In the discrete description of channels, the voltage equation becomes

$$C\frac{dV}{dt} = I - \left[\overline{g_K}(V - E_K)\frac{{N_K}^o}{N_K} + \overline{g_{Na}}(V - E_{Na})\frac{{N_{Na}}^o}{N_{Na}} + g_L(V - E_L)\right]. \tag{13}$$

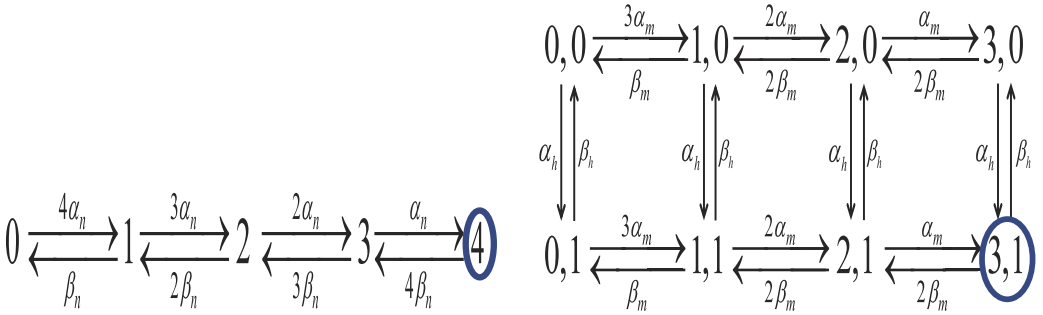

Figure 7. The transition diagram for the K^+ channel (**A**) and for the Na^+ channel (**B**). The numbers in these nodes stand for the numbers of open subunits. (**A**) The number marked with circle is the state in which all four subunits are open. (**B**) A sodium channel is open only when it is in state (3, 1), in which represents the three m subunits and one h subunit are all open.

For the K^+ channel the four n subunits define a transition diagram of five channel states, while for Na^+ channel the three m subunits and one h subunit define a transition diagram of eight channel states. The associated Markov kinetic scheme is depicted in Fig. 7.

Here the voltage-dependent transition rates read[1]

$$\begin{aligned}
\alpha_n &= \frac{0.01(V+55)}{1-\exp[-(V+55)/10]},\ \beta_n = 0.125\exp[-(V+65)/80],\\
\alpha_m &= \frac{0.1(V+40)}{1-\exp[-(V+40)/10]},\ \beta_m = 4\exp[-(V+65)/18],\\
\alpha_h &= 0.07\exp[-(V+65)/20],\ \beta_h = \frac{1}{1+\exp[-(V+35)/10]}.
\end{aligned} \tag{14}$$

For subunits m and n, the opening rates increase and the closing rates decrease as the membrane voltage increases, while the opposite is true for subunit h.

Individual trajectories of this discrete-state Markov process can be generated exactly using the Gillespie algorithm[28], in which the waiting time between transitions is sampled from an exponential distribution and the channel number in each state is updated once a specific transition is selected. However the transition rates depend on the membrane voltage, and therefore change over time. If the time between the transition from one state to another is far less than the characteristic voltage variation time, the voltage can be assumed to be fixed during transitions.

A Markov process can be described with master equation, which directly evolves probability distribution in the state space of a system based on specific interstate transition rates. The usually large set of master equations could be recast into a QFT form in which the probability evolution is governed by a wave equation while the field theoretic formulation is equivalent to a generating function approach[40].

For example, for an elementary reaction such as $A \rightleftharpoons B$, we denote by $P(m, n)$ the probability of having m A's and n B's, the master equation is

$$\begin{aligned}
\frac{dP}{dt}(m,n) &= k[-mP(m,n) + (m+1)P(m+1,n-1)]\\
&\quad + k_[-nP(m,n) + (n+1)P(m-1,n+1)]
\end{aligned} \tag{15}$$

where k and $k\_$ are the forward and backward reaction rates. If the total number of A, B is large, there would be many equations, each for a particular (m, n) state. However, they can be transformed into one single PDE for the generating function $\Psi(x, y, t) = \sum_{m,n} P(m, n, t)x^m y^n$,

$$\frac{\partial\Psi}{\partial t} = k(y-x)\frac{\partial\Psi}{\partial x} + k\_(x-y)\frac{\partial\Psi}{\partial y}. \tag{16}$$

The exact analytic solution can be obtained using the method of characteristics. A solution of generating function eq. (16) reads

$$\Psi(x, y, t) = (xf_{11}(t) + yf_{21}(t))^{m_0}(xf_{12}(t) + yf_{22}(t))^{n_0} \tag{17}$$

where m_0 and n_0 are initial numbers of A and B. x and y are just symbolic variables of A and B, and f_{ij} satisfies the equation

$$\begin{cases} \dot{f}_{1i} &= k\_f_{2i} - kf_{1i} \\ \dot{f}_{2i} &= kf_{1i} - k\_f_{2i} \end{cases} \tag{18}$$

and the initial condition $f(0) = 1$, being an identity matrix.

Linear noise approximation. All the computation and analysis are based on eq. (4) about the stochastic membrane voltage dynamics with the channel based description, and we could substitute the local $\langle V\rangle$ for V till the width of voltage distribution meets the threshold. Linear noise approximation may be used to compute the width of membrane voltage distribution. Firstly, we assume that

$$N_K{}^o = \langle N_K{}^o\rangle + \xi_1,\ N_{Na}{}^o = \langle N_{Na}{}^o\rangle + \xi_2$$

as in the linear noise approximation[36], with the Gaussian white noise specified by

$$\langle \xi_1(t)\xi_1(t')\rangle = \Gamma_1\delta(t-t'),\ \langle \xi_2(t)\xi_2(t')\rangle = \Gamma_2\delta(t-t') \tag{19}$$

where Γ_1 and Γ_1 are defined in eqs (5 and 6), leading to a Langevin equation of V

$$\begin{aligned} \frac{dV}{dt} &= \frac{1}{C}\left[I - \left[\overline{g_K}(V-E_K)\frac{\langle N_K{}^o\rangle}{N_K} + \overline{g_{Na}}(V-E_{Na})\frac{\langle N_{Na}{}^o\rangle}{N_{Na}} + g_L(V-E_L)\right]\right] \\ &\quad - \frac{\overline{g_K}}{CN_K}(V-E_K)\xi_1 - \frac{\overline{g_{Na}}}{CN_{Na}}(V-E_{Na})\xi_2 \\ &\equiv A(V) + g_1(V)\xi_1 + g_2(V)\xi_2. \end{aligned} \tag{20}$$

The corresponding Fokker-Planck equation is

$$\frac{\partial P(V,t)}{\partial t} = -\frac{\partial}{\partial V}(A(V)P) + \frac{1}{2}\frac{\partial^2}{\partial V^2}[(\Gamma_1 g_1{}^2 + \Gamma_2 g_2{}^2)P], \tag{21}$$

from which one obtains equations for the first and second moment of V

$$\begin{aligned} \partial_t\langle V\rangle &= \langle A(V)\rangle \\ &= \frac{1}{C}\left[I - \left[\overline{g_K}(\langle V\rangle - E_K)\frac{\langle N_K{}^o\rangle}{N_K} + \overline{g_{Na}}(\langle V\rangle - E_{Na})\frac{\langle N_{Na}{}^o\rangle}{N_{Na}} + g_L(\langle V\rangle - E_L)\right]\right], \end{aligned} \tag{22}$$

$$\begin{aligned} \partial_t\sigma_V{}^2 &= \left[\Gamma_1\frac{\overline{g_K}^2}{C^2N_K{}^2} + \Gamma_2\frac{\overline{g_{Na}}^2}{C^2N_{Na}{}^2} - \frac{2}{C}\left(\overline{g_K}\frac{\langle N_K{}^o\rangle}{N_K} + \overline{g_{Na}}\frac{\langle N_{Na}{}^o\rangle}{N_{Na}} + g_L\right)\right]\sigma_V{}^2 \\ &\quad + \Gamma_1\frac{\overline{g_K}^2}{C^2N_K{}^2}(\langle V\rangle - E_K)^2 + \Gamma_2\frac{\overline{g_{Na}}^2}{C^2N_{Na}{}^2}(\langle V\rangle - E_{Na})^2. \end{aligned} \tag{23}$$

References

1. Hodgkin, A. L. & Huxley, A. F. A quantitative description of membrane current and its application to conduction and excitation in nerve. *J. Physiol.* **117,** 500–544 (1952).
2. Wiesenfeld, K. & Moss, F. Stochastic resonance and the benefits of noise: from ice ages to crayfish and SQUIDs. *Nature* **373,** 33–36 (1995).
3. McCormick, D. A. Spontaneous Activity: Signal or Noise? *Science* **285,** 541–543 (1999).
4. Faisal, A. A., Selen, L. P. J. & Wolpert, D. M. Noise in the nervous system. *Nat. Rev. Neurosci.* **9,** 292–303 (2008).
5. Wang, Q. Y., Zheng, Y. H. & Ma, J. Cooperative dynamics in neuronal networks. *Chaos, Solitons & Fractals* **56,** 19C–27 (2013).
6. Wang, Q. Y., Chen, G. R. & Perc, M. Synchronous Bursts on Scale-Free Neuronal Networks with Attractive and Repulsive Coupling. *PLoS one* **6,** e15851 (2011).
7. Wang, Q. Y., Zhang, H. H. & Chen, G. R. Stimulus-induced transition of clustering firings in neuronal networks with information transmission delay. *Eur. Phys. J. B* **86,** 301 (2013).
8. Wang, Q. Y., Xia, S. & Chen, G. R. Delay-induced synchronization transition in small-world Hodgkin-Huxley neuronal networks with channel blocking. *DCDS-B* **16,** 607–621 (2011).
9. Sun, X. J., Perc, M., Lu, Q. S. & Kurths, J. Spatial coherence resonance on diffusive and small-world networks of Hodgkin-Huxley neurons. *CHAOS* **18,** 023102 (2008).
10. Sun, X. J., Lei, J. Z., Perc, M., Lu, Q. S. & Lv, S. J. Effects of channel noise on firing coherence of small-world Hodgkin-Huxley neuronal networks. *Eur. Phys. J. B* **79,** 61C–66 (2011).
11. Ozer, M., Perc, M. & Uzuntarla, M. Controlling the spontaneous spiking regularity via channel blocking on Newman-Watts networks of Hodgkin-Huxley neurons. *EPL* **86,** 40008 (2009).
12. White, J. A., Rubinstein, J. T. & Kay, A. R. Channel noise in neurons. *Trends Neurosci.* **23,** 131–137 (2000).
13. Goldwyn, J. H. & Shea-Brown, E. The What and Where of Adding Channel Noise to the Hodgkin-Huxley Equations. *PLoS Comput. Biol.* **7,** e1002247 (2011).
14. Hänggi, P. Stochastic Resonance in Biology: How Noise Can Enhance Detection of Weak Signals and Help Improve Biological Information Processing. *ChemPhysChem.* **3,** 285–290 (2002).
15. Chow, C. C. & White, J. A. Spontaneous action potentials due to channel fluctuations. *Biophys J.* **71,** 3013–3021 (1996).

16. Schneidman, E., Freedman, B. & Segev, I. Ion Channel Stochasticity May Be Critical in Determining the Reliability and Precision of Spike Timing. *Neural Comput.* **10,** 1679–1703 (1998).
17. Hoffman, D. A., Magee, J. C. & Colbert, C. M. K^+ channel regulation of signal propagation in dendrites of hippocampal pyramidal neurons. *Nature* **387,** 869–875 (1998).
18. Brunel, N., Chance, F. S., Fourcaud, N. & Abbott, L. F. Effects of Synaptic Noise and Filtering on the Frequency Response of Spiking Neurons. *Phys.Rev. Lett.* **86,** 2186–2189 (2001).
19. Manwani, A. & Koch, C. Detecting and estimating signals in noisy cable structures. *Neural Comput.* **11,** 1797–C1829 (1999).
20. Zhang, H. H., Wang, Q. Y., Perc, M. & Chen, G. R. Synaptic plasticity induced transition of spike propagation in neuronal networks. *Commun. Nonlinear Sci Numer. Simulat.* **18,** 601–C615 (2013).
21. Imennov, N. S. & Rubinstein, J. T. Stochastic population model for electrical stimulation of the auditory nerve. *IEEE Trans. Biomed. Eng.* **10,** 2493–2501 (2009).
22. Saarinen, A., Linne, M. L. & Yli-Harja, O. Stochastic differential equation model for cerebellar granule cell excitability. *PLoS Comput. Biol.* **4,** e1000004 (2008).
23. Rowat, P. Interspike interval statistics in the stochastic Hodgkin-Huxley model: Coexistence of gamma frequency bursts and highly irregular firing. *Neural Comput.* **19,** 1215–1250 (2007).
24. Skaugen, E. & Walloe, L. Firing behaviour in a stochastic nerve membrane model based upon the Hodgkin-Huxley equations. *Acta Physiolo. Scand.* **107,** 343–363 (1979).
25. White, J. A., Klink, R., Alonso, A. & Kay, A. R. Noise from voltage-gated ion channels may influence neuronal dynamics in the entorhinal cortex. *J. Neurophysiol.* **80,** 262–269 (1998).
26. Steinmetz, P. N., Manwani, A. & Koch, C. Subthreshold Voltage Noise due to Channel Flu tuations in A tive Neuronal Membranes. *J. Comput. Neurosci.* **9,** 133C48 (2000).
27. Jung, P. & Shuai, J. W. Optimal sizes of ion channel clusters. *Europhys. Lett.* **56,** 29–35 (2001).
28. Gillespie, D. T. Exact stochastic simulation of coupled chemical reactions. *J. Phys. Chem.* **81,** 2340–2361 (1977).
29. Fox, R. F. & Lu, Y. N. Emergent collective behavior in large numbers of globally coupled independently stochastic ion channels. *Phys. Rev. E.* **49,** 3421–3431 (1994).
30. Fox, R. F. Stochastic versions of the hodgkin-huxley equations. *Biophys. J.* **72,** 2068–2074 (1997).
31. Huang, Y. D., Li, X. & Shuai, J. W. Langevin approach with rescaled noise for stochastic channel dynamics in Hodgkin-Huxley neuron. *Chin. Phys. B* **24,** 120501 (2015).
32. Orio, P. & Soudry, D. Simple, fast and accurate implementation of the diffusion approximation algorithm for stochastic ion channels with multiple states. *PLoS One* **7,** e36670 (2012).
33. Dangerfield, C. E., Kay, D. & Burrage, K. Modeling ion channel dynamics through reflected stochastic differential equations. *Phys. Rev. E* **85,** 051907 (2012).
34. Huang, Y. D., Rdiger, S. & Shuai, J. W. Channel-based Langevin approach for the stochastic Hodgkin-Huxley neuron. *Phys. Rev. E* **87,** 012716 (2012).
35. Huang, Y. D., Rdiger, S. & Shuai, J. W. Accurate Langevin approaches to simulate Markovian channel dynamics. *Phys. Biol.* **12,** 061001 (2015).
36. Van Kampen, N. G. *Stochastic process in physics and chemistry*, Vol. 1 (Elsevier, 1992).
37. Lan, Y. & Papoian, G. A. Stochastic Resonant Signaling in Enzyme Cascades. *Phys. Rev. Lett.* **98,** 228301 (2007).
38. Lan, Y. & Papoian, G. A. Evolution of complex probability distributions in enzyme cascades. *J. Theor. Bio.* **248,** 537–545 (2007).
39. Lan, Y. & Papoian, G. A. The interplay between discrete noise and nonlinear chemical kinetics in a signal amplification cascade. *J. Chem. Phys.* **125,** 154901 (2006).
40. Lan, Y., Wolynes, P. G. & Papoian, G. A. A variational approach to the stochastic aspects of cellular signal transduction. *J. Chem. Phys.* **125,** 124106 (2006).
41. Lan, Y., Elston, T. C. & Papoian, G. A. Elimination of fast variables in chemical Langevin equations. *J. Chem. Phys.* **129,** 214115 (2008).
42. Huxley, A. From overshoot to voltage clamp. *Trends. Neurosci.* **25,** 553–558 (2002).
43. Linaro, D., Storace, M. & Giugliano, M. Accurate and Fast Simulation of Channel Noise in Conductance-Based Model Neurons by Diffusion Approximation. *PLoS Comput. Biol.* **7,** e1001102 (2011).
44. Sengupta, B., Laughlin, S. B. & Niven, J. E. Comparison of Langevin and Markov channel noise models for neuronal signal generation. *Phys. Rev. E.* **81,** 011918 (2010).

Acknowledgements

This research is supported by the National Natural Science Foundation of China (Grant No. 11375093, Grant No. 31370830), MOST 2013CB922000 of the National Key Basic Research Program of China and the China National Funds for Distinguished Young Scholars (Grant No. 11125419).

Author Contributions

Y.H.L. conceived the study and actively participated in modifying the text, A.Q.L. performed the analytic computation and wrote the manuscript. A.Q.L., Y.D.H. and J.W.S. did the numerical calculation and A.Q.L. drew the figures. All authors approved the final version of the manuscript.

Additional Information

Competing financial interests: The authors declare no competing financial interests.

How to cite this article: Ling, A. *et al.* Channel based generating function approach to the stochastic Hodgkin-Huxley neuronal system. *Sci. Rep.* **6**, 22662; doi: 10.1038/srep22662 (2016).